

Highly Stable Molecular Borromean Rings

Ye Lu,^a Yue-Jian Lin,^a Zhen-Hua Li^a and Guo-Xin Jin^{*,a}

^a State Key Laboratory of Molecular Engineering of Polymers, Collaborative Innovation Center of Chemistry for Energy Materials, Department of Chemistry, Fudan University, Shanghai, 200433, P. R. China

A series of Cp*Rh-based molecular Borromean rings (BRs) are prepared from naphthazarine or metallaligand. Some of as-synthesized BRs display high stability and are formed in high yields in solution. The reason is related to the length ratio of the long-arm linker and short-arm linker, where smaller aspect ratios of the metallarectangles promote improved stability and yields of the BRs in solution. Increasing the width of the metallaligand or pyridyl ligand hinders the formation of BRs and leads to unoccupied monomeric rectangles, which were further used as catalysts for the acyl transfer reaction between *N*-acetylimidazole and (4-(pyridin-4-yl)phenyl) methanol.

Keywords Borromean rings, Metallarectangles, Self-assembly, Supramolecular chemistry, Density functional calculations

Introduction

In the past two decades, a wide range of topologically fascinating interlocked molecules have prepared by coordination-driven self-assembly,¹ such as Borromean rings,² Solomon links,³ star of David catenanes,⁴ pentafoil knots,⁵ and others.⁶ One intriguing and challenging synthetic target in this field is the family of molecular Borromean rings (BRs), which consist of three chemically independent rings that are locked in such a way that no two of the three rings are linked with each other.^{2a,7} The first BRs structure prepared by “all-in-one” synthetic strategies was reported by Stoddart and coworker in 2004, and was based on metal ion templates.⁸ After that, our group presented a template-free self-assembly method for synthesizing BRs based on Cp*Rh (Cp* = pentamethylcyclopentadienyl) and Cu(II) metallaligand in 2013.⁹ Recently, other BRs based on template-free self-assembly are synthesized by our group and Chi's group, constructed by half-sandwich metal units (Rh, Ir or Ru).¹⁰ Moreover, we further established a stepwise separation method for *p*-dihalobenzenes based on BRs.¹¹ As research continues, a number of new problems attracted our interest. For example, the BRs built by dihalogenated or tetracene-based bridge ligand showed modest stability and yield in solution, which is reduced further by dilution, solvent or guest molecules,^{10a,11} thus, how can we prepare the BRs with high stability and high yield in solution? What is the relationship between stability and structure in BRs? Meanwhile, we established earlier that the formation of BRs is related to the length of long-arm linker and short-arm linker.^{9b} However, after forming

the BRs structure, what kind of special properties could be engineered into the BRs by altering this aspect ratio?

In fact, our original intention for using Cu(II) metallaligand was to construct discrete metallarectangles with two coordinatively-unsaturated metal ions for synergistic catalysis.¹² Compared with metal-organic frameworks, the unique advantage of metallarectangles is that the distance between two catalytic centers can be conveniently adjusted according to the size of the substrate molecule.¹³ However, by increasing the distance between the two open Cu(II) ions, BRs were formed, hampering the catalysis for larger substrates. Thus, for this application, the size of metallarectangles should be retained to hinder the formation of BRs. Though guest or solvent molecules could force the BRs to convert to the corresponding monomeric rectangle (MR) assembly, these guest or solvent molecules would bind inside the metallarectangles and impede further catalysis.^{9b} Therefore, we have to explore other methods to achieve unoccupied MR assemblies, in order to maintain the distance between two open Cu(II) ions.

Herein, we reported a series of Cp*Rh-based BRs prepared by pyridyl ligand and various binuclear precursor. Those precursor is bridged by naphthazarine, metallaligand [Pd(opba)]²⁻ [opba = *o*-phenylenebis(oxamato)] or metallaligand [Cu(nabo)]²⁻ [nabo = 2,3-naphthalenebis(oxamato)]. Some of these BRs display high stability and are formed in high yields in solution. The reason is perhaps related to the length ratio of the long-arm linker and short-arm linker, where smaller aspect ratios of the metallarectangles could promote improved stability and yields of the BRs in solution.

This article has been accepted for publication and undergone full peer review but has not been through the copyediting, typesetting, pagination and proofreading process, which may lead to differences between this version and the Version of Record. Please cite this article as doi: 10.1002/cjoc.201700590

Meanwhile, increasing the width of the metallaligand or pyridyl ligand hindered the formation of those highly stable BRs and led to unoccupied MRs. Thus, these MRs were further used in catalysis on larger substrates, for example, the acyl-transfer reaction between *N*-acetylimidazole and (4-(pyridin-4-yl)phenyl) methanol.

Experimental

Preparation of II-BRs. A CH₃OH solution of [Cp*RhCl₂]₂ (124 mg, 0.2 mmol) was added to a solution of naphthazarine (38 mg, 0.2 mmol) and NaOH (16 mg, 0.4 mmol) in CH₃OH (40 mL), and the suspension was stirred at room temperature for 6 h. AgOTf (102.8 mg, 0.4 mmol) was added to the mixture and stirred for 3 h, followed by filtration to remove insoluble compounds (AgCl and NaCl). 4,4'-Bipyridylacetylene (40.8 mg, 0.2 mmol) was then added to the filtrate. After the solution was stirred at room temperature for 12 h, the reaction mixture was concentrated to a volume of 3 mL under reduced pressure, filtered through Celite and recrystallized by slow diffusion of diethyl ether into the filtrate. A green crystalline solid was obtained in 88.6% yield (206.7 mg); ¹H NMR (400 MHz, CD₃OD, ppm): δ = 9.04 (d, *J* = 5.6 Hz, 24H, Py-H), 7.30 (d, *J* = 5.6 Hz, 24H, Py-H), 6.70 (s, 24H, naphthazarine-H), 1.69 (s, 180H, Cp*); Anal. Calcd for C₂₇₆H₂₅₂F₃₆N₁₂O₆₀Rh₁₂S₁₂: C 47.35, H 3.63, N 2.40, found: C 47.31, H 3.64, N 2.43; ESI-MS *m/z*: [II-BRs - 3OTf]³⁺ calcd. 2184.11, found 2184.11; [II-BRs - 4OTf]⁴⁺ calcd. 1600.84, found 1600.84; IR (KBr disk, cm⁻¹) *ν* = 1604, 1533, 1488, 1416, 1270, 1224, 1157, 1031, 963, 854, 836, 638, 548, 518, 445.

Preparation of 3a. A CH₃OH solution of [Cp*RhCl₂]₂ (124 mg, 0.2 mmol) was added to a solution of K₂[Pd(opba)] (86.4 mg, 0.2 mmol) in CH₃OH (40 mL), and the suspension was stirred at room temperature for 1 h. AgOTf (102.8 mg, 0.4 mmol) was then added to the mixture, and this was stirred for 6 h followed by filtration to remove insoluble compounds (AgCl and NaCl). 4,4'-bipyridine (L₁) (31.2 mg, 0.2 mmol) was then added to the filtrate. After the solution was stirred at room temperature for 12 h, the reaction mixture was concentrated to a volume of 3 mL under reduced pressure, filtered through Celite and recrystallized by slow diffusion of diethyl ether into the filtrate. An orange crystalline solid was obtained in 91.6% yield (235.4 mg); ¹H NMR (400 MHz, CD₃OD and *d*₆-DMSO, ppm): δ = 8.70 (d, *J* = 6.4 Hz, 8H, Py-H), 8.21 (d, *J* = 6.4 Hz, 8H, Py-H), 8.18 (d, *J* = 6.0 Hz, 4H, obpa-H), 7.27 (t, 4H, obpa-H), 1.72 (s, 60H, Cp*); Anal. calcd for C₈₄H₈₄F₁₂N₈O₂₄Pd₂Rh₄S₄: C 39.25, H 3.29, N 4.36, found: C 39.20, H 3.27, N 4.33; IR (KBr disk, cm⁻¹) *ν* = 1610, 1581, 1470, 1420, 1383, 1343, 1278, 1224, 1160, 1072, 1031, 819, 759, 638, 587, 517, 462.

Preparation of 4a-BRs. The synthesis of 4a-BRs was carried out similarly to that of 3a with the use of

4,4'-bipyridylacetylene (L₂) (40.8 mg, 0.2 mmol) instead of 4,4'-bipyridine (L₁). 4a was obtained as a yellow solid in a 92.3% yield (246.1 mg); ¹H NMR (400 MHz, CD₃OD ppm): δ = 8.80 (d, *J* = 5.6 Hz, 12H, Py-H), 8.70 (d, *J* = 5.6 Hz, 12H, Py-H), 8.33 (d, *J* = 8.0 Hz, 6H, obpa-H), 8.07 (d, *J* = 8.0 Hz, 6H, obpa-H), 7.76 (d, *J* = 5.6 Hz, 12H, Py-H), 6.98 (d, *J* = 5.6 Hz, 12H, Py-H), 6.78 (t, 6H, obpa-H), 6.59 (t, 6H, obpa-H), 1.79 (s, 90H, Cp*), 1.74 (s, 90H, Cp*); Anal. calcd for C₂₇₆H₂₅₂F₃₆N₂₄O₇₂Pd₆Rh₁₂S₁₂: C 41.44, H 3.18, N 4.20, found: C 41.43, H 3.15, N 4.18; ESI-MS *m/z*: [4a-BRs - 3OTf]³⁺ calcd. 2517.24, found 2517.24; [4a-BRs - 4OTf]⁴⁺ calcd. 1850.69, found 1850.69; IR (KBr disk, cm⁻¹) *ν* = 1606, 1581, 1471, 1422, 1383, 1342, 1261, 1225, 1202, 1161, 1031, 834, 759, 639, 587, 518, 502, 461.

Preparation of 4b-BRs. The synthesis of 4b-BRs was carried out similarly to that of 4a-BRs with the use of Na₂[Cu(opba)] (71.4 mg, 0.2 mmol) instead of K₂[Pd(opba)]. 4b was obtained as a green solid in a 90.8% yield (234.3 mg); Anal. calcd for C₂₇₆H₂₅₂F₃₆N₂₄O₇₂Cu₆Rh₁₂S₁₂: C 42.82, H 3.28, N 4.34, found: C 42.81, H 3.25, N 4.31; IR (KBr disk, cm⁻¹) *ν* = 1608, 1576, 1461, 1412, 1384, 1348, 1261, 1225, 1202, 1168, 1035, 837, 751, 639, 587, 517, 502, 462.

Preparation of 5a-BRs. The synthesis of 5a was carried out similarly to that of 3a with the use of 1,4-di(pyridin-4-yl)benzene (L₃) (46.4 mg, 0.2 mmol) instead of 4,4'-bipyridine (L₁). 5a-BRs was obtained as a yellow solid in a 93.8% yield (255.4 mg); ¹H NMR (400 MHz, CD₃OD, ppm): δ = 9.37 (d, *J* = 5.6 Hz, 6H, Py-H), 9.31 (d, *J* = 5.6 Hz, 6H, Py-H), δ = 9.02 (d, *J* = 5.6 Hz, 6H, Py-H), 8.87 (d, *J* = 5.6 Hz, 6H, Py-H), 8.56 (d, *J* = 8.0 Hz, 6H, Py-H), 8.21 (d, *J* = 5.6 Hz, 6H, Py-H), 8.09 (d, *J* = 8.0 Hz, 6H, obpa-H), 7.82 (d, *J* = 8.0 Hz, 6H, obpa-H), 7.01 (d, *J* = 5.6 Hz, 6H, Py-H), 6.83 (br, 6H, phenyl-H), 6.82 (d, *J* = 8.0 Hz, 6H, Py-H), 6.81 (t, 6H, obpa-H), 6.54 (t, 6H, obpa-H), 6.41 (br, 6H, phenyl-H), 5.22 (br, 6H, phenyl-H), 5.15 (br, 6H, phenyl-H), 1.88 (s, 90H, Cp*), 1.73 (s, 90H, Cp*); Anal. calcd for C₂₈₈H₂₇₆F₃₆N₂₄O₇₂Pd₆Rh₁₂S₁₂: C 42.35, H 3.41, N 4.12, found: C 42.36, H 3.39, N 4.15; ESI-MS *m/z*: [5a-BRs - 5OTf]⁵⁺ calcd. 1484.81, found 1484.80; [5a-BRs - 6OTf]⁶⁺ calcd. 1212.01, found 1212.03; IR (KBr disk, cm⁻¹) *ν* = 1609, 1581, 1421, 1258, 1224, 1156, 1030, 817, 756, 638, 586, 518, 460.

Preparation of 6b. The synthesis of 6b was carried out similarly to that of 4b-BRs with the use of 1,4-bis(4-pyridyl)naphthalene (L₄) (56.4 mg, 0.2 mmol) instead of 4,4'-bipyridylacetylene (L₂). 6b was obtained as a green solid in a 90.5% yield (247.7 mg); Anal. calcd for C₁₀₄H₉₆Cu₂F₁₂N₈O₂₄Rh₄S₄: C 45.64, H 3.54, N 4.09, found: C 45.66, H 3.53, N 4.10; ESI-MS *m/z*: [6b - 2OTf]²⁺ calcd. 1219.55, found 1219.57; [6a-BRs - 4OTf]⁴⁺ calcd. 1850.69, found 1850.69; IR (KBr disk, cm⁻¹) *ν* = 1617, 1587, 1471, 1419, 1278, 1224, 1161, 1031, 638, 573, 517, 463.

Preparation of 7a-BRs. The synthesis of 7a-BRs

was carried out similarly to that of **3a** with the use of *N,N'*-di-4-pyridinyloxalamide (**L₅**) (48.4 mg, 0.2 mmol) instead of 4,4'-bipyridine (**L₁**). **7a-BRs** was obtained as a yellow solid in a 91.1% yield (249.8 mg); Anal. calcd for C₂₆₄H₂₆₄F₃₆N₃₆O₈₄Pd₆Rh₁₂S₁₂: C 38.54, H 3.23, N 6.13, found: C 38.55, H 3.25, N 6.14; ESI-MS *m/z*: [**7a-BRs** – 3OTf]³⁺ calcd. 2593.26, found 2593.26; [**7a-BRs** – 4OTf]⁴⁺ calcd. 1907.71, found 1907.70; IR (KBr disk, cm⁻¹) ν = 1712, 1611, 1582, 1504, 1485, 1425, 1259, 1161, 1031, 639, 574, 518, 460.

Preparation of 8a-BRs. The synthesis of **8a-BRs** was carried out similarly to that of **3a** with the use of *N,N'*-bis(4-pyridyl)terephthalamide (**L₆**) (63.6 mg, 0.2 mmol) instead of 4,4'-bipyridine (**L₁**). **8a-BRs** was obtained as a yellow solid in a 88.9% yield (257.3 mg); Anal. calcd for C₃₀₀H₂₈₈F₃₆N₃₆O₈₄Pd₆Rh₁₂S₁₂: C 41.49, H 3.34, N 5.81, found: C 41.47, H 3.35, N 5.80; IR (KBr disk, cm⁻¹) ν = 1661, 1610, 1580, 1515, 1420, 1280, 1256, 1163, 1031, 639, 518, 460.

Preparation of 9b. The synthesis of **9b** was carried out similarly to that of **4b-BRs** with the use of *N,N'*-bis(4-pyridyl)-1,4,5,8-naphthalenetetracarboxydiimide (**L₇**) (84.0 mg, 0.2 mmol) instead of 4,4'-bipyridylacetylene (**L₂**). **9b** was obtained as a green solid in a 92.1% yield (277.5 mg); ESI-MS *m/z*: [**9b** – 3OTf]³⁺ calcd. 855.03, found 855.03; Anal. calcd for C₁₁₂H₉₂Cu₂F₁₂N₁₂O₃₂Rh₄S₄: C 44.65, H 3.08, N 5.58, found: C 44.66, H 3.09, N 5.56; IR (KBr disk, cm⁻¹) ν = 1721, 1681, 1618, 1584, 1419, 1347, 1250, 1160, 1030, 766, 638, 517.

Preparation of 10a. The synthesis of **10a** was carried out similarly to that of **5a-BRs** with the use of K₂[Pd(nabo)] (96.0 mg, 0.2 mmol) instead of K₂[Pd(opba)]. **10a** was obtained as a yellow solid in a 89.5% yield (252.6 mg); ¹H NMR (400 MHz, CD₃OD and *d*₆-DMSO, ppm): δ = 8.64 (s, 4H, nabo-H), δ = 8.62 (d, *J* = 5.4 Hz, 8H, Py-H), 8.00 (d, *J* = 5.6 Hz, 8H, Py-H), 7.97 (m, 4H, obpa-H), δ = 7.95 (d, *J* = 2.8 Hz, 8H, phenyl-H), 7.58 (t, 4H, obpa-H), 1.76 (s, 60H, Cp*); Anal. calcd for C₁₀₄H₉₆F₁₂N₈O₂₄Pd₂Rh₄S₄: C 44.25, H 3.43, N 3.97, found: C 44.23, H 3.45, N 3.96; IR (KBr disk, cm⁻¹) ν = 1607, 1583, 1484, 1460, 1423, 1262, 1030, 1009, 756, 638, 517, 474.

Preparation of 10b. The synthesis of **10b** was carried out similarly to that of **10a** with the use of Na₂[Cu(nabo)] (81.0 mg, 0.2 mmol) instead of K₂[Pd(nabo)]. **10b** was obtained as a green solid in a 89.1% yield (243.7 mg); ESI-MS *m/z*: [**10b** – 3OTf]³⁺ calcd. 763.05, found 763.05; Anal. calcd for C₁₀₄H₉₆Cu₂F₁₂N₈O₂₄Rh₄S₄: C 45.64, H 3.54, N 4.09, found: C 45.66, H 3.55, N 4.08; IR (KBr disk, cm⁻¹) ν = 1608, 1590, 1456, 1422, 1384, 1258, 1224, 1160, 1031, 638, 518, 475.

Preparation of 11b-BRs. The synthesis of **11b-BRs** was carried out similarly to that of **10b** with the use of 2,6-di(pyridin-4-yl)naphthalene (**L₈**) (56.4 mg, 0.2 mmol) instead of 1,4-bis(4-pyridyl)-naphthalene (**L₄**). **11b-BRs** was obtained as a green solid in a 93.2% yield

(264.4 mg); ESI-MS *m/z*: [**11b-BRs** – 6OTf]⁶⁺ calcd. 1269.40, found 1269.41; Anal. calcd for C₃₃₆H₃₀₀Cu₆F₃₆N₂₄O₇₂Rh₁₂S₁₂: C 47.42, H 3.55, N 3.95, found: C 47.40, H 3.58, N 3.91; IR (KBr disk, cm⁻¹) ν = 1617, 1589, 1473, 1422, 1384, 1268, 1224, 1160, 1031, 638, 573, 518, 463.

Crystallographic Details. Crystallographic data for complexes **3a**, **II-BRs**, **5a-BRs**, **7a-BRs** were collected at 203 K, 150 K or 173 K using a CCD-Bruker APEX DUO system (Mo K α , λ = 0.71073 Å). Those of **4a-BRs**, **4b-BRs**, **6b**, **8a-BRs**, **9b**, **11b-BRs** were collected at 173 K or 150 K using a Bruker D8 VENTURE micro-focus X-ray source system (Cu K α , λ = 1.54178 Å). Indexing was performed using APEX 2 (difference vectors method). Data integration and reduction were performed using SaintPlus 6.01. Absorption correction was performed by the multiscan method implemented in SADABS. The structures were solved and refined using SHELXTL-97. The single-crystal X-ray diffraction data of **3a**, **II-BRs**, **4a-BRs**, **4b-BRs**, **5a-BRs**, **6b**, **7a-BRs**, **8a-BRs**, **9b** and **11b-BRs** have been deposited in the Cambridge Crystallographic Data Centre under accession number CCDC: 1537126 (**3a**), 1537136 (**4a-BRs**), 1552228 (**II-BRs**), 1537137 (**4b-BRs**), 1537141 (**5a-BRs**), 1537143 (**6b**), 1537142 (**7a-BRs**), 1537144 (**8a-BRs**), 1537139 (**9b**) and 1537140 (**11b-BRs**).

Results and discussion

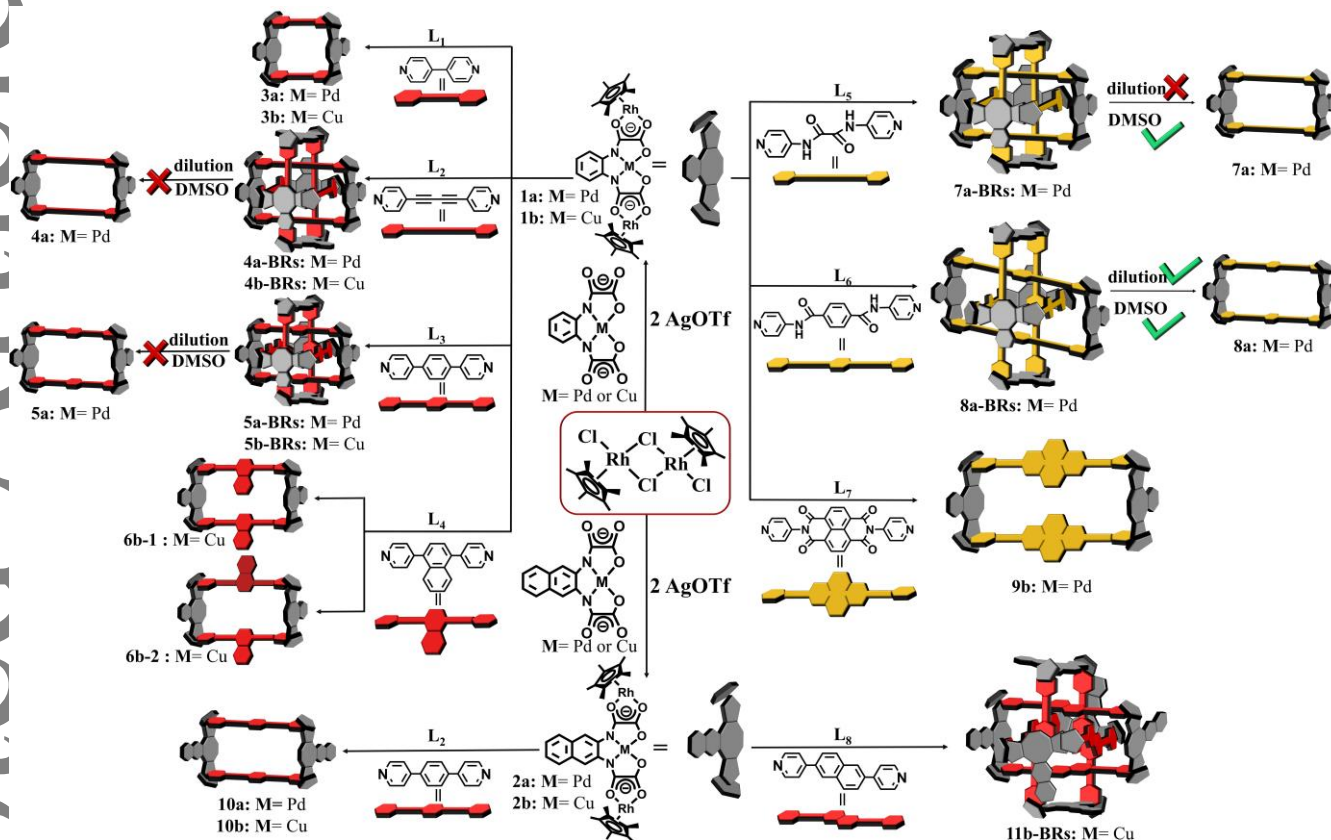
The relationship between stability and structure in BRs. Our research group has a longstanding interest in the self-assembly of two preorganized binuclear half-sandwich metal (Rh or Ir) molecular clips and pyridyl ligands, which led us to attempt similar reactions with Pd(II) metallaligand in order to avoid the paramagnetic Cu(II) nuclei used in previous studies.^{7,14} Thereby, a solution of dirhodium precursor **1a** based on [Pd(opba)]²⁻ (1.0 equiv) reacts with **L₁** (**L₁** = 4,4'-bipyridine) (1.0 equiv), leading to exclusive formation of a tetranuclear metallarectangle **3a** (Scheme 1). Single-crystal X-ray crystallographic analysis confirmed the structure of **3a** to be a discrete MR (Figure S46) and analyzed by NMR spectroscopy (Figure S1-S4).

The formation of BRs based on [Cu(opba)]²⁻ is related to the length of pyridyl ligand.^{9a} Hence, we attempted to use the longer (and linear) bipyridyl ligand **L₂** (**L₂** = 4,4'-bipyridylacetylene) to build a metallarectangle (**4a-BRs**, Scheme 1 and Figure 1) with precursor **1a**. Gratifyingly, orange block crystals of **4a-BRs** were isolated in a 92.3% yield upon crystallization by diffusion of diethyl ether into a methanol solution (including several drops of DMSO). The single-crystal X-ray crystallographic analysis established **4a-BRs** to have a discrete BRs structure (Figure 2a and Figure S47a), which is further checked by ESI-MS (Figure S60-S61). In the structure of **4a-BRs**, the metallaligand unit [Pd(opba)]²⁻, displays a planar structure and the distance from the carbon atoms of the alkynyl group to

the $[\text{Pd}(\text{opba})]^{2-}$ plane is ca. 3.5 Å, which is accordance with the conventional distance of π - π interactions. It is worth noting that, for **4a-BRs**, the length of the long arm minus the length of short arm is less than 7 Å, which is double the conventional distance of π - π interactions. Hence, in order to achieve the optimal distance for π - π interactions, the long arm of **4a-BRs** had to

curve inward. As is shown in Figure 2c, the short arm of **4a-BRs** is ca. 10.8 Å, while the distance between two corresponding alkynyl groups is only ca. 9.5 Å. A similar situation was also observed for **4b-BRs** (Figure S47-S49), which was built using $[\text{Cu}(\text{opba})]^{2-}$ and **L₂** (Scheme 1).

Scheme 1. Synthesis of metallarectangles and interconversion between BRs and MR



In order to discover the relationship between the aspect ratio and properties, we attempt to keep the long-arm linker and shorten the short-arm linker. A shorter dirhodium precursor **I** based on naphthazarine is used to construct metallarectangles with **L₂**, and named **II-BRs** (Figure 1). Single-crystal X-ray crystallographic analysis and ESI-MS confirmed the BRs structure of **II-BRs** (Figure 2b, S50, S62 and S63). The distance from the carbon atoms of the alkynyl group to the naphthazarine plane is ca. 3.4 Å, which is also accordance with the conventional distance of π - π interactions. In contrast to **4a-BRs**, for **II-BRs**, the length of the long arm minus the length of short arm is more than 7 Å, so that the long arm of **II-BRs** had to curve outward to achieve the optimal distance for π - π interactions, the short arm of **II-BRs** is ca. 8.3 Å, while the distance between two corresponding alkynyl groups is ca. 9.3 Å (Figure 2d). Actually, BRs could be obtained by further shortening the short-arm linker. Very recently, we reported the BRs based on dihalogenated ligands, which is also constructed by **L₂**, but their dirhodium precursor is bridged by fluoranilic acid,

chloranilic acid and bromianilic acid, and then, the length of their short-arm linker is only ca. 7.9 Å (Figure S51).¹¹

Three kinds of BRs, **4a-BRs**, **II-BRs** and the BRs based on dihalogenated ligands, have the same long-arm linker and different short-arm linker (Table S12). At this point, we considered the possibility that different properties could be caused by the dissimilarity between the structures. The BRs based on dihalogenated ligands showed modest stability and yield in methanol solution, which is reduced further by dilution. However, **II-BRs** showed very different behavior. The ¹H NMR spectra of **II-BRs** in methanol solution displayed one groups of metallarectangle signals (Figure S5), which is checked by ¹³C NMR, ¹H-¹H ROESY NMR and DOSY NMR (Figure S6-S8). Moreover, with the dilution, no new signals were found, even if the concentration have diluted to 0.5mM (Figure S9). That means there are no balance between BRs and corresponding MR in methanol solution of **II-BRs** and **II-BRs** present stronger stability than the BRs based on dihalogenated ligand in solution.¹¹ Then, upon increasing the ratio of *d*₆-DMSO in CD₃OD,

a clear signal attributable to the corresponding MR, **II**, was observed (Figure S10-S11), and further confirmed by ^{13}C NMR, ^1H - ^1H ROESY NMR and DOSY NMR (Figure S12-S14).¹⁵ When the $\text{CD}_3\text{OD}:d_6\text{-DMSO}$ ratio is 5:4, **II-BRs** was found to be completely transformed to the corresponding MR **II** (Figure S10).

Compared with **II-BRs** and the BRs based on dihalogenated ligands, **4a-BRs** have the same long-arm linker and longest short-arm linker. The behavior of **4a-BRs** in solution is also different with the former two. The ^1H NMR spectra of **4a-BRs** in methanol displayed two groups of metallarectangle signals in a 1:1 ratio (Figure S15), not one group, checked by ^{13}C NMR, and ^1H - ^1H ROESY NMR (Figure S16-S18). Furthermore, the ratio of the two groups of signals remained unchanged under different concentrations (Figure S19), and two groups of signals were confirmed to belong to one complex due to their identical diffusion coefficients observed via DOSY NMR (Figure S20). The reason of two group signal maybe is due to the smaller aspect ratio and higher symmetry cannot be achieved in this situation. Meanwhile, with the decrease of aspect ratios, **4a-BRs** display higher stability than **II-BRs**, when the $\text{CD}_3\text{OD}:d_6\text{-DMSO}$ ratio is 5:4, there is no new signal found in **4a-BRs** (Figure S19), **4a-BRs** is immune to DMSO. This higher stability in solution may be attributed to the length ratio of the long-arm and short-arm linkers.

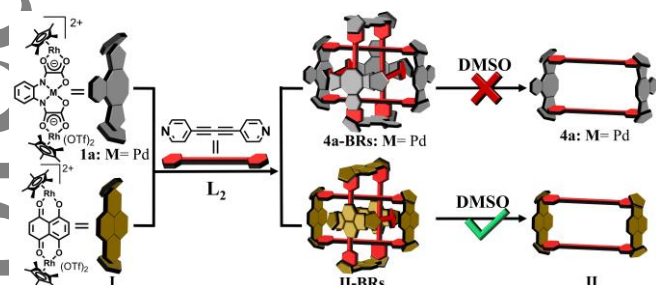


Figure 1. Synthesis and conversion of **4a-BRs**, **4a**, **II-BRs** and **II**.

In order to further prove this, the aspect ratios of the metallarectangles were decreased again. **5a-BRs** was prepared using precursors **1a** and shorter pyridyl ligands **L₃** (**L₃** = 1,4-di(pyridin-4-yl)benzene) by the same method (Scheme 1). Single-crystal X-ray crystallographic analysis and ESI-MS confirmed the BRs structure of **5a-BRs** (Figure S52-S53 and Figure S64-S65). Similar to **4a-BRs**, for **5a-BRs**, the length of the long arm minus the length of short arm is also less than 7 Å, the long arm of **5a-BRs** was found to curve inward, too (Figure S52 and Table S12). Hence, the NMR spectra of **5a-BRs** in methanol also displayed two groups of metallarectangle signals in a 1:1 ratio (Figure S21-S26), and these two groups of signals have the same diffusion constants (Figure S23). And then, **5a-BRs** also displays excellent stability in solution. The BR structure is immune to dilution, and addition of DMSO (Figure S27). DFT binding energy calculations were performed to further find out the difference of **4a-BRs** and **5a-BRs** on stability. The computational results showed that the binding energy between

the three MRs of **5a-BRs** (−217.3 kcal/mol) is much lower than that of **4a-BRs** (−147.4 kcal/mol) (Table S1, Figure S74-S75). These results further underscore our contention that metallarectangles with smaller aspect ratios could help to increase the stability of BRs structures.

BRs also could be built by the interactions between Cu(II) centers of the metallaligand and carbonyl groups of the pyridyl ligand. In contrast to Cu(II), Pd(II) centers only have four coordination sites and their axial coordination ability is very weak. We were also interested in testing whether BRs could be formed by the interaction between tetracoordinate Pd(II) centers and carbonyl groups. More importantly, what effect does the aspect ratios of metallarectangle have on the stability of this kind of BRs? To address those problems, two kinds of pyridyl ligand with carbonyl group, **L₅** and **L₆** (**L₅** = *N,N'*-di-4-pyridinyloxalamide and **L₆** = *N,N'*-bis(4-pyridyl)terephthalamide), were used to construct metallarectangle with precursor **1a**, respectively, resulting in the formation of two new compounds **7a-BRs** (based on **L₅**) and **8a-BRs** (based on **L₆**) (Scheme 1). The single-crystal X-ray crystallographic analysis indicated **7a-BRs** and **8a-BRs** to have a discrete BRs structure (Figure 3, Figure S54, Figure S55 and Table S12). The BRs structure of **7a-BRs** was further confirmed by ESI-MS (Figure S66-S67).

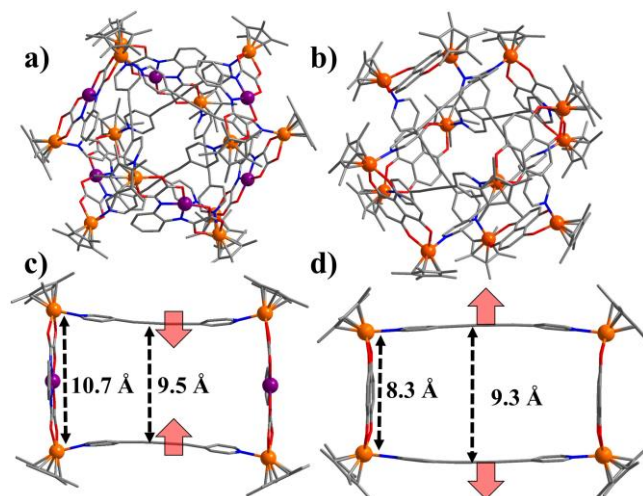


Figure 2. Single-crystal X-ray structures of (a) **4a-BRs**, (b) **II-BRs**, (c) the metallarectangle of **4a-BRs** and (d) the metallarectangle of **II-BRs** (N, blue; O, red; C, gray; Rh, orange; Pd, violet). Hydrogen atoms and counter anions are omitted for clarity.

The size of the metallarectangles of **7a-BRs** is similar to that of **5a-BRs**, and the long arm of the metallarectangle was also found to curve inward (Figure 3c and Table S12). The distance between the Pd(II) center and the corresponding oxygen atom of the carbonyl group was found to be ca. 3.6 Å (Figure S56). In methanol solution, the **7a-BRs** also displayed similar properties to **5a-BRs**. The spectra of **7a-BRs** present two groups of metallarectangle signals in a 1:1 ratio (Figure S28-S31), and these two groups of signals have the same diffusion constants (Figure S32). The BRs structure of **7a-BRs** is also

immune to changes in concentration (Figure S33). But, upon increasing the ratio of d_6 -DMSO in CD_3OD , new peaks were observed in 1H NMR spectrum, along with peaks from **7a-BRs**, that indicated the formation of a new compound (**7a**; Figure S34). The 1H NMR signal of the new compound **7a** presented an MR structure (Figure S34), which was confirmed by a 1H DOSY spectrum (Figure S35). However, even in pure d_6 -DMSO (5.0 mM), the BRs structure of **7a-BRs** cannot be completely transformed to the corresponding MR (Figure S34). Despite the similar size of their metallarectangles, **5a-BRs** is immune to d_6 -DMSO, but **7a-BRs** is not. This means that the axial position of Pd(II) and the carbonyl group plays a very important role in the formation of **7a-BRs**.

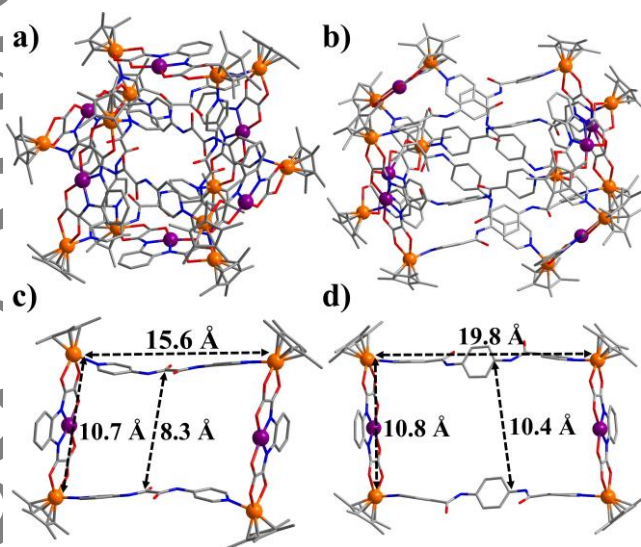


Figure 3. Single-crystal X-ray structures of: (a) **7a-BRs**, (b) **8a-BRs**, (c) the metallarectangle of **7a-BRs** and (d) the metallarectangle of **8a-BRs** (N, blue; O, red; C, gray; Rh, orange; Pd, violet). Hydrogen atoms and counter anions are omitted for clarity.

Compared with **7a-BRs**, the aspect ratios of the metallarectangles in **8a-BRs** is obviously larger than that in **7a-BRs** (Figure 3d and Table S12). For **8a-BRs**, the distance between the Pd atom and the corresponding oxygen of carbonyl group is only ca. 3.1 Å (Figure S57), which is significantly shorter than this distance in **7a-BRs**. This indicated that the interaction between the Pd(II) atom and the carbonyl group in **8a-BRs** is stronger than that in **7a-BRs**. Interestingly, **8a-BRs** display lower stability in solution than **7a-BRs**. The 1H NMR spectrum of **8a-BRs** is very cluttered and difficult to confidently assign (Figure S36). However, upon increasing the ratio of d_6 -DMSO to CD_3OD , a clear signal attributable to the corresponding MR, **8a**, was observed (Figure S37-40). Moreover, when the $CD_3OD:d_6$ -DMSO ratio is 5:4 (5.0 mM), **8a-BRs** was found to be completely transformed to the corresponding MR **8a**. However, for **7a-BRs**, even if in pure d_6 -DMSO (5.0 mM), the BR structure cannot be completely transformed to corresponding MR. Furthermore, the BRs structure of **8a-BRs** could be destroyed by dilution (Figure S41). Therefore, unless the interaction between Pd(II) and carbonyl group, the length ratio of the

long-arm and short-arm linkers also contributed to the formation of BRs. DFT binding energy calculations were performed to further confirm the relationship between the stability of BRs and the aspect ratio in this kind of BRs: the binding energy between the three MRs of **7a-BRs** (–217.5 kcal/mol) is stronger than that of **8a-BRs** (–192.3 kcal/mol) (Table S1, Figure S76-S77). These results underline that metallarectangles with smaller aspect ratios could help to increase the stability of BRs structures in solution, both for BRs based on π - π stacking or those based on interactions between Pd(II) centers and carbonyl groups.

Increasing the width of ligands. Metallarectangles based on $[Cu(opba)]^{2-}$ and pyridyl ligands are promising catalysts. However, by lengthening the distance between the two Cu(II) ions, BRs are formed, impeding catalysis with larger substrates. Moreover, some of these BRs display high stability in solution. Thus, how to maintain the distance between the two open Cu(II) centers and achieve an empty MR? We sought to increase the width of the linker ligand (the details see catalytic activity studies in supporting information).

We chose **L₄** (**L₄** = 1,4-bis(4-pyridyl)naphthalene) to construct a metallarectangle (**6b**) with precursor **1b** as **L₄** is the same length as **L₃**, but significantly wider (Scheme 1). As predicted, the structure of **6b** is a discrete MR, which was confirmed by single-crystal X-ray crystallographic analysis (Figure 4) and ESI-MS (Figure S68). A pair of conformational isomers were found to exist in the crystal, denoted **6b-1** (naphthalene groups facing in the same direction) and **6b-2** (naphthalene groups facing in opposite directions). **L₇** (**L₇** = *N,N*-bis(4-pyridyl)-1,4,5,8-naphthalenetetracarboxydiimide) was also used to construct the metallarectangle **9b** under similar conditions. Similarly to **L₆**, **L₇** also bears suitable carbonyl groups for coordination, and while both are of similar lengths, **L₇** is wider than **L₆** (Scheme 1). **9b** is a discrete MR, as confirmed by single-crystal X-ray crystallographic analysis (Figure S58) and ESI-MS (Figure S69).

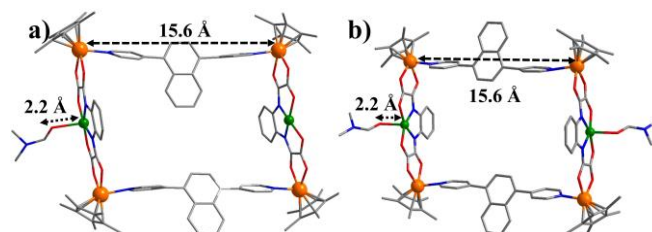


Figure 4. Single-crystal X-ray crystal structures of: (a) **6b-1** and (b) **6b-2** (N, blue; O, red; C, gray; Rh, orange; Cu, green). Hydrogen atoms and counter anions are omitted for clarity. The distance between the Cu(II) atom and the oxygen atom of DMF is ca. 2.2 Å, DMF is added during the recrystallization process.

We reasoned that increasing the width of the metallaligand could similarly hinder the formation of BRs. Dirhodium precursors **2a** and **2b** were thus prepared using $[Pd(nabo)]^{2+}$ and $[Cu(nabo)]^{2+}$, respectively. The only difference between nabo and obpa is that a naphthyl

group replaces the phenylene group of the latter (Scheme 1). As predicted, the structure of **10b** is also a discrete MR, which is confirmed by ESI-MS (Figure S70). In order to further prove the MR structure, **10a** was prepared from **2a** and **L₃** for NMR spectroscopic characterization. The NMR results of **10a** showed typical signals for the MR structure, and only one group of metallarectangle signals (Figure S42-S45).

Moreover, if the long arm was further lengthened, the BRs structure could be obtained once again, for example in the case of **11b-BRs**, which is constructed from precursors **2b** and **L₈** (**L₈** = 2,6-di(pyridin-4-yl)naphthalene) (Scheme 1). Its BRs structure is confirmed by the X-ray structures and ESI-MS (Figure S59 and S71). This fact further underscores the relationship between the formation of BRs and the width of the ligand.

The catalytic acyl transfer reaction. After obtaining the MR **6b** and **10b**, which are larger than those reported previously,⁹ We attempted to use them as catalysts for the acyl transfer reaction with larger substrates. We reasoned that the NAI and (4-(pyridin-4-yl)phenyl)methanol substrates could achieve optimal orientation and alignment for highly efficient acyl transfer by binding within the cavity of the metallacycle through the open Cu centers. Furthermore, only a combination of substrates with the right distance can span the cavity and react at an accelerated rate. As is shown in Figure S72, both **6b** and **10b** significantly accelerate the reaction rate, which may be ascribed to **6b** and **10b** having highly favorable cavity sizes for accommodating the two reactants. These results also prove that the structure of **10b** is indeed a discrete MR. At the same time, the reaction rate of **6b** is slightly lower than that of **10b** because of the conformational isomer (**6b-1** and **6b-2**). **5b-BRs** was found to inefficiently catalyze the reaction as there is no space for substrate entry into the BR structure. However, the cavity of **3b** is inherently too narrow for (4-(pyridin-4-yl)phenyl)methanol. These findings lead to the postulate that the nitrogen atoms of NAI and (4-(pyridin-4-yl)phenyl)methanol can easily coordinate to the inner Cu centers of **6b** and **10b**, forming the cooperatively-bound intermediate with low activation energy, thus facilitating the subsequent catalytic cycle (Figure S73).

Conclusions

We have prepared a series of Cp*Rh-based BRs from various binuclear precursors. Through experiments and theoretical calculations, we found that the stability of the BRs is associated with the length ratio of the long-arm and short-arm linkers, with smaller aspect ratios leading to improved stability and yield of the BRs in solution. By increasing the width of the metallaligand or pyridyl ligand, the formation of BRs was hindered and MR could be obtained. These MR have the similar sizes to the metallarectangles of corresponding BRs. With the appropriate cavity size, MR **6b** and **10b** show remarkable catalytic

abilities with high efficiency in the acyl transfer reaction between NAI and (4-(pyridin-4-yl)phenyl)methanol. We hope that our results will help to deepen the understanding and awareness of complicated interlocked structure, and advance the field of supramolecular assembly chemistry.

Acknowledgement

This work was supported by the National Science Foundation of China (21531002, 21720102004), the Program for Changjiang Scholars and Innovative Research Team in University (IRT-15R12) and the Shanghai Science Technology Committee (13JC1400600) and China Postdoctoral Science Foundation (2015M581517); GXJ thanks the Alexander von Humboldt Foundation for a Humboldt Research Award.

References

- (a) Raymo, F. M.; Stoddart, J. F. *Chem. Rev.* **1999**, *99*, 1643; (b) Forgan, R. S.; Sauvage, J. P.; Stoddart, J. F. *Chem. Rev.* **2011**, *111*, 5434; (c) Ramirez, G. G.; Leigh, D. A.; Stephens, A. J. *Angew. Chem. Int. Ed.* **2015**, *54*, 6110; (d) Berl, V.; Huc, I.; Khoury, R. G.; Krische, M. J.; Lehn, J. M. *Nature* **2000**, *407*, 720; (e) Cook, T. R.; Stang, P. J. *Chem. Rev.* **2015**, *115*, 7001; (f) Smulders, M. M. J.; Riddell, I. A.; Browne, C.; Nitschke, J. R. *Chem. Soc. Rev.* **2013**, *42*, 1728; (g) Klosterman, J. K.; Yamauchi, Y.; Fujita, M. *Chem. Soc. Rev.* **2009**, *38*, 1714; (h) Han, M.; Engelhard, D. M.; Clever, G. H. *Chem. Soc. Rev.* **2014**, *43*, 1848; (i) Gianneschi, N. C.; Masar, M. S.; Mirkin, C. A. *Acc. Chem. Res.* **2005**, *38*, 825; (j) Vogtle, F.; Dunnwald, T.; Schmidt, T. *Acc. Chem. Res.* **1996**, *29*, 451; (k) Xue, M.; Yang, Y.; Chi, X. D.; Yan X. Z.; Huang F. H. *Chem. Rev.* **2015**, 7398.
- (a) Cantrill, S. J.; Chichak, K. S.; Peters, A. J.; Stoddart, J. F. *Acc. Chem. Res.* **2005**, *38*, 1; (b) Meyer, C. D.; Forgan, R. S.; Chichak, K. S.; Peters, A. J.; Tangchaivang, N.; Cave, G. W. V.; Khan, S. I.; Cantrill, S. J.; Stoddart, J. F. *Chem-Eur. J.* **2010**, *16*, 12570.
- (a) Song, Y. H.; Singh, N.; Jung, J.; Kim, H.; Kim, E. H.; Cheong, H. K.; Kim, Y.; Chi, K. W. *Angew. Chem. Int. Ed.* **2016**, *55*, 2007; (b) Schouwey, C.; Holstein, J. J.; Scopelliti, R.; Zhurov, K. O.; Nagornov, K. O.; Tsybin, Y. O.; Smart, O. S.; Bricogne, G.; Severin, K. *Angew. Chem. Int. Ed.* **2014**, *53*, 11261; (c) Beves, J. E.; Danon, J. J.; Leigh, D. A.; Lemonnier, J. F.; Vitorica-Yrezabal, I. J. *Angew. Chem. Int. Edit.* **2015**, *54*, 7555; (d) Ibukuro, F.; Fujita, M.; Yamaguchi, K.; Sauvage, J. P. *J. Am. Chem. Soc.* **1999**, *121*, 11014; (e) Prakasam, T.; Lusi, M.; Elhabiri, M.; Platas-Iglesias, C.; Olsen, J. C.; Asfari, Z.; Cianferani-Sanglier, S.; Debaene, F.; Charbonniere, L. J.; Trabolsi, A. *Angew. Chem. Int. Edit.* **2013**, *52*, 9956.
- Leigh, D. A.; Pritchard, R. G.; Stephens, A. J. *Nat. Chem.* **2014**, *6*, 978.
- Marcos, V.; Stephens, A. J.; Jaramillo-Garcia, J.; Nussbaumer, A. L.; Woltering, S. L.; Valero, A.; Lemonnier, J. F.; Vitorica-Yrezabal, I. J. V.; Leigh, D. A. *Science* **2016**, *352*, 1555.
- (a) Danon, J. J.; Kruger, A.; Leigh, D. A.; Lemonnier, J. F.;

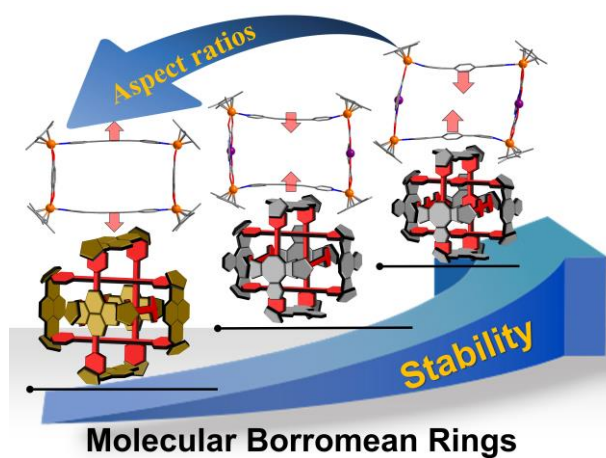
- Stephens, A. J.; Vitorica-Yrezabal, I. J.; Woltering, S. L. *Science* **2017**, *355*, 159; (b) Sawada, T.; Yamagami, M.; Ohara, K.; Yamaguchi, K.; Fujita, M. *Angew. Chem. Int. Edit.* **2016**, *55*, 4519; (c) Fujita, M.; Fujita, N.; Ogura, K.; Yamaguchi, K. *Nature* **1999**, *400*, 52; (d) Lee, H.; Elumalai, P.; Singh, N.; Kim, H.; Lee, S. U.; Chi, K. W. *J. Am. Chem. Soc.* **2015**, *137*, 4674; (e) Zhu, R.; Lubben, J.; Dittrich, B.; Clever, G. H. *Angew. Chem. Int. Edit.* **2015**, *54*, 2796.
- 7 Han, Y. F.; Jin, G. X. *Acc. Chem. Res.* **2014**, *47*, 3571.
- 8 Chichak, K. S.; Cantrill, S. J.; Pease, A. R.; Chiu, S. H.; Cave, G. W. V.; Atwood, J. L.; Stoddart, J. F. *Science* **2004**, *304*, 1308.
- 9 (a) Huang, S. L.; Lin, Y. J.; Hor, T. S. A.; Jin, G. X. *J. Am. Chem. Soc.* **2013**, *135*, 8125; (b) Huang, S. L.; Lin, Y. J.; Li, Z. H.; Jin, G. X. *Angew. Chem. Int. Ed.* **2014**, *53*, 11218.
- 10 (a) Kim, T.; Singh, N.; Oh, J.; Kim, E. H.; Jung, J.; Kim, H.; Chi, K. W. *J. Am. Chem. Soc.* **2016**, *138*, 8368; (b) Singh, N.; Kim, D.; Kim, D. H.; Kim, E. H.; Kim, H.; Lah, M. S.; Chi, K. W. *Dalton Trans.* **2017**, *46*, 571; (c) Zhang, L.; Lin, L.; Liu, D.; Lin, Y. J.; Li, Z. H.; Jin, G. X. *J. Am. Chem. Soc.* **2017**, *139*, 1653.
- 11 Lu, Y.; Deng, Y. X.; Lin, Y. J.; Han, Y. F.; Weng, L. H.; Li, Z. H.; Jin, G. X. *Chem* **2017**, *3*, 110.
- 12 (a) Shultz, A. M.; Farha, O. K.; Hupp, J. T.; Nguyen, S. T. *J. Am. Chem. Soc.* **2009**, *131*, 4204; (b) Yoon, H. J.; Mirkin, C. A. *J. Am. Chem. Soc.* **2008**, *130*, 11590; (c) Yoon, H. J.; Heo, J.; Mirkin, C. A. *J. Am. Chem. Soc.* **2007**, *129*, 14182.
- 13 Deria, P.; Gomez-Gualdron, D. A.; Hod, I.; Snurr, R. Q.; Hupp, J. T.; Farha, O. K. *J. Am. Chem. Soc.* **2016**, *138*, 14449.
- 14 Han, Y. F.; Jin, G. X. *Chem. Soc. Rev.* **2014**, *43*, 2799.
- 15 Vajpayee, V.; Song, Y. H.; Yang, Y. J.; Kang, S. C.; Cook, T. R.; Kim, D. W.; Lah, M. S.; Kim, I. S.; Wang, M.; Stang, P. J.; Chi, K. W. *Organometallics* **2011**, *30*, 6482.

Entry for the Table of Contents

Page No.

Title

Highly Stable Molecular Borromean Rings



A series of Cp*Rh-based molecular Borromean rings (BRs) are prepared from naphthazarine or metallaligand. Smaller aspect ratios of the metallarectangles could promote improved stability and yields of the BRs in solution. Increasing the width of ligand hinders the formation of BRs and leads to unoccupied monomeric rectangles, which were further used as catalysts for the acyl transfer reaction between *N*-acetylimidazole and (4-(pyridin-4-yl)phenyl)methanol.

Ye Lu; Yue-Jian Lin; Zhen-Hua Li and Guo-Xin Jin*

Accepted Article